



Published in final edited form as:

ACS Chem Biol. 2006 October 24; 1(9): 570–574. doi:10.1021/cb600345k.

Turning G proteins on and off using peptide ligands

William W. Ja^{1,†}, Ofer Wiser^{2,†,‡}, Ryan J. Austin¹, Lily Y. Jan², and Richard W. Roberts^{3,*}

¹Division of Biology, California Institute of Technology, Pasadena, CA, 91125, USA

²Howard Hughes Medical Institute, Departments of Physiology and Biochemistry, University of California, San Francisco, 1550 4th Street, San Francisco, CA 94143, USA

³University of Southern California, Department of Chemistry and Mork Family Department of Chemical Engineering, Los Angeles, CA, 90089, USA

Abstract

Intracellular G α subunits represent potential therapeutic targets for a number of diseases. Here we describe three classes of new molecules that modulate G protein signaling by direct targeting of G α . Using mRNA display, we have identified unique peptide sequences that bind G α_{i1} . Functionally, individual peptides were found that either enhance or repress basal levels of G protein-activated inwardly rectifying potassium (GIRK) channel signaling—a downstream effector of G protein activation—indicating that the peptides directly turn G proteins on or off *in vivo*. A third functional class acts as a signaling attenuator—basal GIRK channel activity is unaffected but responses to repeated G protein activation are reduced. These data demonstrate that G protein-directed ligands can achieve similar physiological effects as those resulting from classical receptor targeting and may serve as leads for developing new classes of therapeutics.

Heterotrimeric guanine nucleotide-binding proteins (G proteins), composed of α , β , and γ subunits, play a critical role in communicating extracellular signals to intracellular signal transduction pathways through membrane-spanning G protein-coupled receptors (GPCRs) (1,2). Activation of GPCRs by extracellular agonists triggers the exchange of GDP with GTP in the G α subunit and dissociation of G $\beta\gamma$ heterodimers from G α -GTP, which both regulate multiple effectors. G $\beta\gamma$ subunits, for example, can directly regulate adenylyl cyclase, phospholipase C β isozymes, and GIRK channels (3). GTP hydrolysis by the inherent G α guanosine triphosphatase (GTPase) activity, a reaction catalyzed by various GTPase-activating proteins (GAPs), returns G α to the GDP-bound state and results in reassociation with G $\beta\gamma$ and termination of signaling.

Intracellular G proteins have potential as drug targets for a number of diseases (4–7). The large number of possible combinations of α , β , and γ subunits suggest that direct G protein ligands could affect individual effector pathways and/or modify signaling kinetics with great specificity (5,8,9). The G protein regulatory (GPR) or GoLoco motif, for example, is a peptide guanine nucleotide dissociation inhibitor (GDI) which is implicated in receptor-independent signaling (10,11). Other recent advances include the identification of ligands for G $\beta\gamma$ that affect downstream signaling pathways using peptide (12) or small molecule (13) libraries.

*To whom correspondence should be addressed. richrob@usc.edu.

[†]These authors contributed equally to this work.

[‡]Present address: Goldyne Savad Institute of Gene Therapy, Hadassah University Hospital, P.O. Box 12000, Jerusalem, 91120, Israel

A selection for peptides that bind to G α subunits yields several classes of signaling modulators: activators, inhibitors, and attenuators of G protein signaling.

Supporting Information Available: This material is available free of charge via the Internet.

In vitro peptide selection methods have been widely successful in isolating ligands for biological targets (14,15). Various proteins in the G protein signaling pathway have been targeted by selection libraries, including receptors and $G\alpha$ and $G\beta\gamma$ subunits (8). mRNA display is a selection technique where each peptide in a library is covalently coupled with its encoding mRNA (16,17). Previously, we used mRNA display selection to identify a peptide (R6A) and its core motif (R6A-1) that bind with high affinity and specificity to the GDP-state of $G\alpha$ subunits (18,19). R6A and R6A-1 act as GDIs and compete with $G\beta\gamma$ for binding to $G\alpha_{i1}$ (18,19). We hypothesized that the 9-residue R6A-1 sequence could be used as a scaffold for developing new peptide ligands with different activities and/or specificities for $G\alpha$ subunits. Here we design an mRNA display library based on the R6A-1 core motif and use *in vitro* selection to identify unique peptides that differentially modulate G protein signaling.

A DNA template was constructed to encode the R6A-1 peptide (DQLYWWEYL) flanked by random hexamers on each end (see Methods). Nucleotide incorporation was controlled such that each wild-type residue in the core motif was ~40–50% conserved (20). mRNA display selection was performed on N-terminally biotinylated $G\alpha_{i1}$ (Nb- $G\alpha_{i1}$) due to the previous finding that R6A-derived peptides bind preferentially to Nb- $G\alpha_{i1}$ over the C-terminally biotinylated Cb- $G\alpha_{i1}$ (18). Aluminum fluoride (AIF) was supplemented into the selection buffer to attempt to select for peptides specific for the GDP-AIF state of $G\alpha_{i1}$, a transition state mimic of GTP hydrolysis (21,22). AIF (either as AIF_3 or AIF_4^-) has been shown to activate $G\alpha$ subunits—preventing association with $G\beta\gamma$ heterodimers—and GAPs have been shown to bind exclusively to this transition state mimic. Six rounds of selection were performed and significant binding was observed by the third round (Fig. 1a). Based on the starting library complexity of $\sim 2 \times 10^{13}$ and a maximum enrichment of 10,000-fold per round, we estimate that the third round input pool contained more than 100,000 unique, $G\alpha_{i1}$ -binding peptide sequences. To enrich for peptides specific for the AIF-bound state of $G\alpha_{i1}$, the fifth and sixth round pools were pre-cleared against $G\alpha_{i1}$ -GDP prior to selection against $G\alpha_{i1}$ -GDP-AIF.

DNA sequencing of clones from the sixth round pool showed that the core 9-mer was primarily conserved, except for a preference for Leu instead of Gln in the second position (Fig. 1b and Table 1 in the Supporting Information). The random hexamer regions showed no obvious sequence conservation, although the residues directly flanking the core motif favored several amino acids including Leu, Asp, and Glu. *In vitro* binding assays with individual clones revealed that the peptides bind ~1–40% to immobilized $G\alpha_{i1}$ -GDP-AIF (Fig. 1c). The wide range of binding may suggest that the selection was not complete, or that specificity to the AIF-bound state of $G\alpha_{i1}$ produces a trade-off in overall binding.

Binding assays of individual peptides to $G\alpha_{i1}$ -GDP in the presence or absence of AIF show that most peptides favor the GDP-bound state (Fig. 1c). Hence, the selection identified peptides with a loss of specificity, compared with the original R6A sequence. Only one peptide, AR6-04, exhibited better binding in the presence of AIF, but this peptide appears to have significantly lower affinity for $G\alpha_{i1}$ than other peptides. Because the selected peptides bind both states, pre-clearing the fifth and sixth round pools on $G\alpha_{i1}$ -GDP may have removed the highest affinity peptides while only marginally enriching for specificity to $G\alpha_{i1}$ -GDP-AIF.

AR6-04 and AR6-05 exhibited the highest AIF/GDP-state binding ratios for $G\alpha_{i1}$ and were synthesized for further characterization. Their affinities to immobilized $G\alpha_{i1}$ -GDP were determined by surface plasmon resonance (SPR). Corresponding with the lower binding seen in the *in vitro* assays, the K_D of AR6-04 for $G\alpha_{i1}$ -GDP appears to be $>10 \mu M$. Conversely, AR6-05, with an apparent K_D of ~10 nM, is the highest affinity $G\alpha$ -directed peptide that we have tested, binding more than 6-fold better to $G\alpha_{i1}$ -GDP than our previously described R6A peptide, and more than 20-fold better than the R6A-1 core motif (18). While R6A and R6A-1

show clear 1:1 bimolecular binding kinetics, AR6-05 binding data were well fit only with a more complex kinetics model (Fig. 1 in the Supporting Information).

R6A and R6A-1 were previously shown to compete with G $\beta\gamma$ heterodimers for binding to G α_{i1} *in vitro* (18,19). Binding of radiolabeled G $\beta_1\gamma_2$ to immobilized G α_{i1} in the presence or absence of peptides was performed to determine the peptide effects on G $\beta\gamma$ association. AR6-05 competes with G $\beta\gamma$ for binding to G α_{i1} (Fig. 2a). Like the R6A peptide, binding of G α_{i1} to immobilized AR6-05 precludes G $\beta\gamma$ association (Fig. 2c).

Surprisingly, AR6-04 appears to enhance G $\beta_1\gamma_2$ binding to G α_{i1} . Several *in vitro* assays were performed that support this observation: (1) labeled G $\beta\gamma$ shows higher binding to immobilized G α_{i1} in the presence of free AR6-04 peptide (Fig. 2b), (2) labeled AR6-04 peptide shows 66% higher binding to immobilized G α_{i1} in the presence of G $\beta_1\gamma_2$, and (3) experiments with labeled G $\alpha_{i1}\beta_1\gamma_2$ show that immobilized AR6-04 is able to pull down all three subunits (Fig. 2c).

To test the activity of the peptides in a cellular context, we used a HEK293 cell line expressing the inwardly rectifying potassium channels, GIRK1 and 2, and the dopamine D_{2S} GPCR. Previous cell culture studies have shown that, similar to the G protein specificity observed *in vivo*, only G_{i/o}-coupled receptors activate GIRK channels (23,24). In these cells, GIRK channels are the dominant downstream effectors of released G $\beta\gamma$ subunits. The GPR consensus peptide (10) was previously shown to attenuate signaling events after an initial agonist application, without affecting basal GIRK activity (25). The authors hypothesized that the GPR peptide is able to interact with G α subunits only after an initial activation, which frees G α for peptide binding. We confirmed these results with the L19GPR peptide, which differs from the GPR consensus at a redundant residue (10,18,26). In the absence of peptide, the kinetics of channel deactivation (τ , deactivation time constant) are similar after short (τ_a) followed by long (τ_b) dopamine applications (10.6 ± 1.9 s, $n = 10$ and 13.7 ± 3.4 s, $n = 7$, respectively, $p = 0.68$, Fig. 3a). In contrast, L19GPR increased τ_b significantly compared with controls (Fig. 3b and c). GIRK basal activity returned to its initial values after ~2 min from the dopamine washout, indicating that the L19GPR peptide effect is transient, since a persistent effect should have resulted in higher basal activity.

R6A exhibited similar effects to the L19GPR peptide. R6A increased τ_b moderately while the negative control peptide C-GPR had no effect (Fig. 3d). R6A had minimal effect on the basal GIRK channel activity ($n = 7$, $p = 0.18$) which suggests that, like the GPR peptide, R6A is unable to dissociate G $\alpha\beta\gamma$ heterotrimer *in vivo*. In contrast to R6A, intracellular application of AR6-05 increased basal activity dramatically, suggesting that AR6-05 actively dissociates G $\beta\gamma$ from G α *in vivo* (Fig. 4).

AR6-04 had no effect on the deactivation kinetics (Fig. 3d), but instead directly reduced basal GIRK activity (Fig. 4). This coincides with the *in vitro* binding data, where AR6-04 stabilizes a heterotrimer complex and presumably reduces the active G $\beta\gamma$ available for GIRK channel activation. It is not clear how AR6-04 stabilizes the heterotrimer despite being selected against the G α subunit alone. The peptide sequence differs greatly from the original R6A-1 core motif. The flanking regions of AR6-04, however, share modest sequence similarity to the short G $\beta\gamma$ -binding motifs previously identified (12), suggesting that other molecules that shut down G protein signaling may be constructed by fusing known G α - and G $\beta\gamma$ -specific ligands.

The R6A-1 based peptide library should be useful for the selection of peptides that are specific for various G protein subclasses or nucleotide-bound states. Given the large number of G α_{i1} -binding peptides identified here, unique functions, such as specificity for G α_{i1} over other G α subunits, may have yet to be identified. While it is clear that AR6-04 and AR6-05 affect GIRK channel activity—an effector of G $\beta\gamma$ —the peptide effects on G α -regulated pathways and G α nucleotide-bound states have yet to be determined. For example, because GAPs have been

shown to catalyze GTP hydrolysis by stabilizing a transition state (21,22), selected peptides that bind $G\alpha_{i1}$ -GDP-AIF may act as small molecule GAPs. Although further technological advances are necessary for the facile conversion of peptides to therapeutics, determining the mechanism of action of the AR6-04 and AR6-05 peptides will facilitate the rational design of more potent modulators of G protein signaling for use as biological tools and potential drug leads.

Methods

Materials

Human cDNA clones for G proteins were obtained from the UMR cDNA Resource Center (<http://www.cdna.org>) in the pcDNA3.1+ vector (Invitrogen). The $G\gamma_2$ cDNA vector encoded an N-terminal HA tag. Anti-HA mAb (clone HA-7) was obtained from Sigma. Expression of ^{35}S -Met-labeled G proteins by *in vitro* translation was performed as described previously (19).

mRNA display selection

The doped R6A-1 library was constructed by PCR amplification of oligo 115.1 [5'-AGC AGA CAG ACT AGT GTA ACC GCC (SNN)₆ (S13) (641) (542) (521) (641) (S13) (543) (642) (SNN)₆ CAT TGT AAT TGT AAA TAG TAA TTG TCC C; 1 = 7:1:1:1, 2 = 1:7:1:1, 3 = 1:1:7:1, 4 = 1:1:1:7, A:C:G:T; 5 = 9:1, 6 = 1:9, C:G; N = A, C, G, OR T; S = C OR G (ratios have been adjusted for synthesis incorporation rates)] with primers 47T7FP (5'-GGA TTC TAA TAC GAC TCA CTA TAG GGA CAA TTA CTA TTT ACA ATT AC) and 22.9 (5'-AGC AGA CAG ACT AGT GTA ACC G) to produce dsDNA encoding M-X₆-DQLYWWEYL-X₆-GGYTSLSA, with the core 9-residues conserved ~40–50%. Sequencing of randomly chosen clones from the initial pool revealed a distribution of wild-type residues in the core motif that agreed with theoretical calculations (data not shown). *In vitro* transcription, ligation of the mRNA to the puromycin linker, and purification of the RNA-F30P template were performed as described previously, except that the splint oligo 23.8 (5'-TTT TTT TTT TTN AGC AGA CAG AC) was used for the ligation reaction (18). RNA-peptide fusions were prepared, purified on oligo-dT cellulose, reverse-transcribed with oligo 22.9, and selected against immobilized N-terminally biotinylated $G\alpha_{i1}$ (Nb- $G\alpha_{i1}$) as described previously using a modified selection buffer [25 mM HEPES-KOH at pH 7.5, 150 mM NaCl, 0.05% (v/v) Tween 20, 1 mM β -mercaptoethanol, 10 μM GDP, 20 μM EDTA, 5 mM MgCl_2 , 10 mM NaF, 25 μM AlCl_3 , 0.05% (w/v) BSA, and 1 mg mL^{-1} yeast tRNA] (18).

RNA-peptide fusion binding assay

Purified, RNase-treated mRNA display peptide fusions of individual clones were assayed for binding as described previously (27). Briefly, aliquots of ^{35}S -labeled fusions were added to ~15 μL of Nb- $G\alpha_{i1}$ (~15 μg protein) on streptavidin agarose (immobilized NeutrAvidin on agarose, Pierce) in 1 mL of selection buffer. After binding for 1 h, the matrices were washed with 3×0.6 mL of selection buffer in a 0.45 μm cellulose acetate spin filter (CoStar Spin-X, Corning). Input ^{35}S counts for binding assays were determined by scintillation counting of the washes and the matrix. Bound ^{35}S counts were divided by the input counts to calculate the fraction bound. Binding of RNase-treated peptide fusions to the immobilization matrix alone was less than 0.001. Assays for binding to $G\alpha_{i1}$ -GDP were performed in selection buffer without AIF.

in vitro peptide studies

Peptides were synthesized with the first 3 residues of the C-terminal constant tag (GGY) and purified by Bio-Synthesis, Inc. Three additional C-terminal lysines were added to the AR6-04

peptide to enhance solubility. SPR affinity measurements were made on immobilized Nb-G α_{i1} as described previously (18). Peptide effects on G $\beta\gamma$ association with immobilized Nb-G α_{i1} were assayed by mixing an aliquot of ^{35}S -labeled G $\beta_1\gamma_2$ with ~15 μL of immobilized Nb-G α_{i1} in 1 mL of selection buffer without AIF. After rotating at 4 °C for 1 h, samples were washed with 3 \times 0.6 mL of the binding buffer in a spin filter, as described above. Binding was determined by scintillation counting and scaled to the amount of G $\beta\gamma$ pulled down in the absence of peptide. Data are background subtracted from binding to matrix without immobilized G α_{i1} (~10% of overall binding). AIF reduced G $\beta_1\gamma_2$ pull down on Nb-G α_{i1} to ~50%.

G $\alpha\beta\gamma$ heterotrimer immunoprecipitation

AR6-04 and AR6-05 were expressed as MBP fusion proteins and immobilized by random amine coupling on CNBr-Sepharose 4B (GE Healthcare) as described previously (19). ^{35}S -labeled G $\alpha\beta\gamma$ heterotrimer was immunoprecipitated with anti-HA monoclonal antibody and protein G-sepharose, or pulled down on immobilized MBP as described previously (19). Recovered proteins were separated by SDS-PAGE. Gels were imaged by autoradiography (Storm PhosphorImager, GE Healthcare).

Electrophysiology

We used HEK293 cell lines stably expressing GIRK1, GIRK2a, and the G $_{i/o}$ -coupled dopamine (D $_{2s}$) receptor (23). The pipette solution contained 107 mM KCl, 1.2 mM MgCl $_2$, 1 mM CaCl $_2$, 10 mM EGTA, 5 mM HEPES at pH 7.4, 2 mM MgATP, and 0.3 mM Na $_2$ GTP. Peptides were added to the pipette solution immediately prior to recording. The final DMSO concentration was 0.5% (v/v) or less. The bath solution contained 2.6 mM CaCl $_2$, 1.2 mM MgCl $_2$, 5 mM HEPES at pH 7.4, and either 140 mM KCl (High-K $^+$) or 140 mM NaCl (Zero-K $^+$). Membrane currents were recorded in a whole-cell patch-clamp mode with an Axopatch 200B amplifier (Axon Instruments), and a patch pipette resistance of 2.5–4.5 M Ω . Data were filtered at 1 kHz and digitized at 5 kHz. Cell capacitance was 12–18 pF, and series resistance (5–20 M Ω) was at least 75% compensated on-line. Current recording was acquired after equilibration for ~5 min in gap-free mode at –80 mV. Dopamine (2 μM , Sigma) was applied in bath solution via an N $_2$ -pressurized perfusion system (ALA Scientific Instruments).

Data analysis

Data acquisition and analysis was done by a Digidata 1200A interface (Axon Instruments) and pClamp 8.2 and Microcal Origin 6.0 software. The deactivation time constants (τ) were determined in pClamp (standard exponential). Currents were averaged over 17 ms to reduce 60 Hz background noise. All data are presented as mean \pm s.e.m.. Statistical significance was determined by non-paired, two-tailed student's t tests. In figures: *, $p < 0.05$; **, $p < 0.01$; ***, $p < 0.0001$.

Supplementary Material

Refer to Web version on PubMed Central for supplementary material.

Acknowledgments

We thank D.S. Waugh (National Cancer Institute at Frederick) for providing the original pDW363 vector and P. J. Bjorkman for the use of the Biacore 2000 instrument. This work was supported by funding from the NIH and the Beckman Foundation (R.W.R.), the Howard Hughes Medical Institute and NIMH (L.Y.J.), in the Silvio Conte Center of Neuroscience at UCSF), the European Molecular Biology Organization (O.W.), and a DOD National Defense Science and Engineering Graduate Fellowship (W.W.J.).

References

1. Gilman AG. G proteins: transducers of receptor-generated signals. *Annu. Rev. Biochem* 1987;56:615–649. [PubMed: 3113327]
2. Neves SR, Ram PT, Iyengar R. G protein pathways. *Science* 2002;296:1636–1639. [PubMed: 12040175]
3. Clapham DE, Neer EJ. G protein $\beta\gamma$ subunits. *Annu. Rev. Pharmacol. Toxicol* 1997;37:167–203. [PubMed: 9131251]
4. Nürnberg B, Tögel W, Krause G, Storm R, Breitweg-Lehmann E, Schunack W. Non-peptide G-protein activators as promising tools in cell biology and potential drug leads. *Eur. J. Med. Chem* 1999;34:5–30.
5. Höller C, Freissmuth M, Nanoff C. G proteins as drug targets. *Cell. Mol. Life Sci* 1999;55:257–270. [PubMed: 10188585]
6. Freissmuth M, Waldhoer M, Bofill-Cardona E, Nanoff C. G protein antagonists. *Trends Pharmacol. Sci* 1999;20:237–245. [PubMed: 10366866]
7. Spiegel AM, Weinstein LS. Inherited diseases involving G proteins and G protein-coupled receptors. *Annu. Rev. Med* 2004;55:27–39. [PubMed: 14746508]
8. Ja WW, Roberts RW. G-protein-directed ligand discovery with peptide combinatorial libraries. *Trends Biochem. Sci* 2005;30:318–324. [PubMed: 15950876]
9. Chahdi A, Daeffler L, Gies JP, Landry Y. Drugs interacting with G protein α subunits: selectivity and perspectives. *Fundam. Clin. Pharmacol* 1998;12:121–132. [PubMed: 9565765]
10. Peterson YK, Bernard ML, Ma H, Hazard S III, Graber SG, Lanier SM. Stabilization of the GDP-bound conformation of $G_{i\alpha}$ by a peptide derived from the G-protein regulatory motif of AGS3. *J. Biol. Chem* 2000;275:33193–33196. [PubMed: 10969064]
11. Willard FS, Kimple RJ, Siderovski DP. Return of the GDI: the GoLoco motif in cell division. *Annu. Rev. Biochem* 2004;73:925–951. [PubMed: 15189163]
12. Scott JK, Huang SF, Gangadhar BP, Samoriski GM, Clapp P, Gross RA, Taussig R, Smrcka AV. Evidence that a protein-protein interaction 'hot spot' on heterotrimeric G protein beta gamma subunits is used for recognition of a subclass of effectors. *EMBO J* 2001;20:767–776. [PubMed: 11179221]
13. Bonacci TM, Mathews JL, Yuan C, Lehmann DM, Malik S, Wu D, Font JL, Bidlack JM, Smrcka AV. Differential targeting of $G\beta\gamma$ -subunit signaling with small molecules. *Science* 2006;312:443–446. [PubMed: 16627746]
14. Dower WJ, Mattheakis LC. *In vitro* selection as a powerful tool for the applied evolution of proteins and peptides. *Curr. Opin. Chem. Biol* 2002;6:390–398. [PubMed: 12023121]
15. Lin H, Cornish VW. Screening and selection methods for large-scale analysis of protein function. *Angew. Chem. Int. Edit* 2002;41:4402–4425.
16. Roberts RW, Szostak JW. RNA-peptide fusions for the in vitro selection of peptides and proteins. *Proc. Natl. Acad. Sci. U.S.A* 1997;94:12297–12302. [PubMed: 9356443]
17. Takahashi TT, Austin RJ, Roberts RW. mRNA display: ligand discovery, interaction analysis and beyond. *Trends Biochem. Sci* 2003;28:159–165. [PubMed: 12633996]
18. Ja WW, Roberts RW. *In vitro* selection of state-specific peptide modulators of G protein signaling using mRNA display. *Biochemistry* 2004;43:9265–9275. [PubMed: 15248784]
19. Ja WW, Adhikari A, Austin RJ, Sprang SR, Roberts RW. A peptide core motif for binding to heterotrimeric G protein α subunits. *J. Biol. Chem* 2005;280:32057–32060. [PubMed: 16051611]
20. LaBean TH, Kauffman SA. Design of synthetic gene libraries encoding random sequence proteins with desired ensemble characteristics. *Protein Sci* 1993;2:1249–1254. [PubMed: 8401210]
21. Berman DM, Kozasa T, Gilman AG. The GTPase-activating protein RGS4 stabilizes the transition state for nucleotide hydrolysis. *J. Biol. Chem* 1996;271:27209–27212. [PubMed: 8910288]
22. Tesmer JGG, Berman DM, Gilman AG, Sprang SR. Structure of RGS4 bound to AlF_4^- -activated $G_{i\alpha 1}$: Stabilization of the transition state for GTP hydrolysis. *Cell* 1997;89:251–261. [PubMed: 9108480]

23. Leaney JL, Milligan G, Tinker A. The G protein α subunit has a key role in determining the specificity of coupling to, but not the activation of, G protein-gated inwardly rectifying K^+ channels. *J. Biol. Chem* 2000;275:921–929. [PubMed: 10625628]
24. Benians A, Leaney JL, Tinker A. Agonist unbinding from receptor dictates the nature of deactivation kinetics of G protein-gated K^+ channels. *Proc. Natl. Acad. Sci. U.S.A* 2003;100:6239–6244. [PubMed: 12719528]
25. Webb CK, McCudden CR, Willard FS, Kimple RJ, Siderovski DP, Oxford GS. D2 dopamine receptor activation of potassium channels is selectively decoupled by $G\alpha_i$ -specific GoLoco motif peptides. *J. Neurochem* 2005;92:1408–1418. [PubMed: 15748159]
26. Peterson YK, Hazard S III, Graber SG, Lanier SM. Identification of structural features in the G-protein regulatory motif required for regulation of heterotrimeric G-proteins. *J. Biol. Chem* 2002;277:6767–6770. [PubMed: 11756403]
27. Ja WW, Olsen BN, Roberts RW. Epitope mapping using mRNA display and a unidirectional nested deletion library. *Protein Eng. Des. Sel* 2005;18:309–319. [PubMed: 15980016]

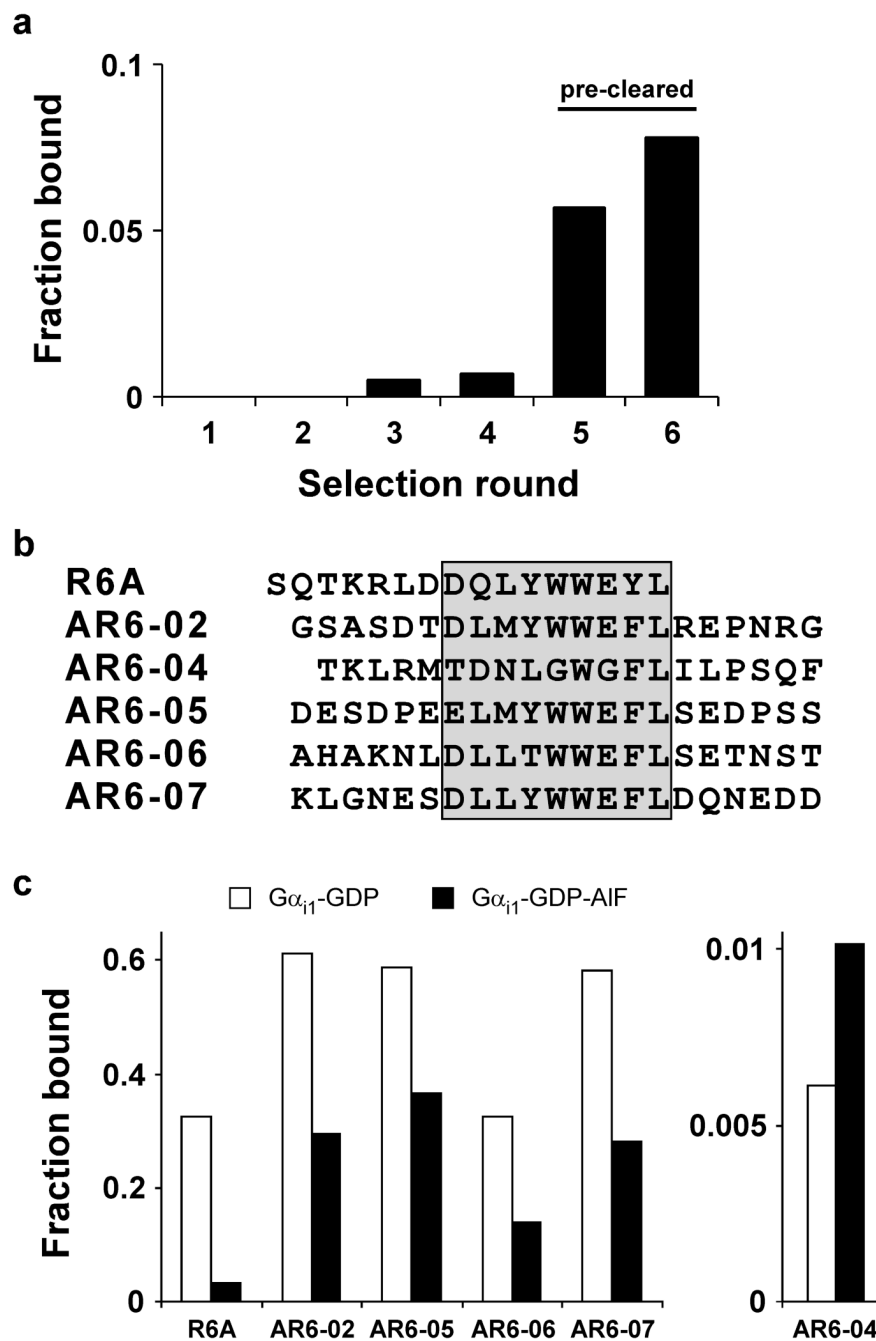


Figure 1. *In vitro* selection targeting Gα_{i1}-GDP-AIF. (a) Fraction of ³⁵S-Met-labeled mRNA display pools from each round of selection bound to immobilized Gα_{i1}-GDP-AIF and recovered by elution with SDS. The inputs for the fifth and sixth rounds were pre-cleared against Gα_{i1}-GDP prior to selection. (b) Sequences of peptides used in *in vitro* studies. The region corresponding to the R6A-1 core motif is boxed (grey). The C-terminal constant region is not shown. (c) Binding of individual, RNase-treated, ³⁵S-Met-labeled mRNA display fusions to Gα_{i1}-GDP or Gα_{i1}-GDP-AIF. Except for AR6-04, all tested peptides have a preference for binding to Gα_{i1}-GDP.

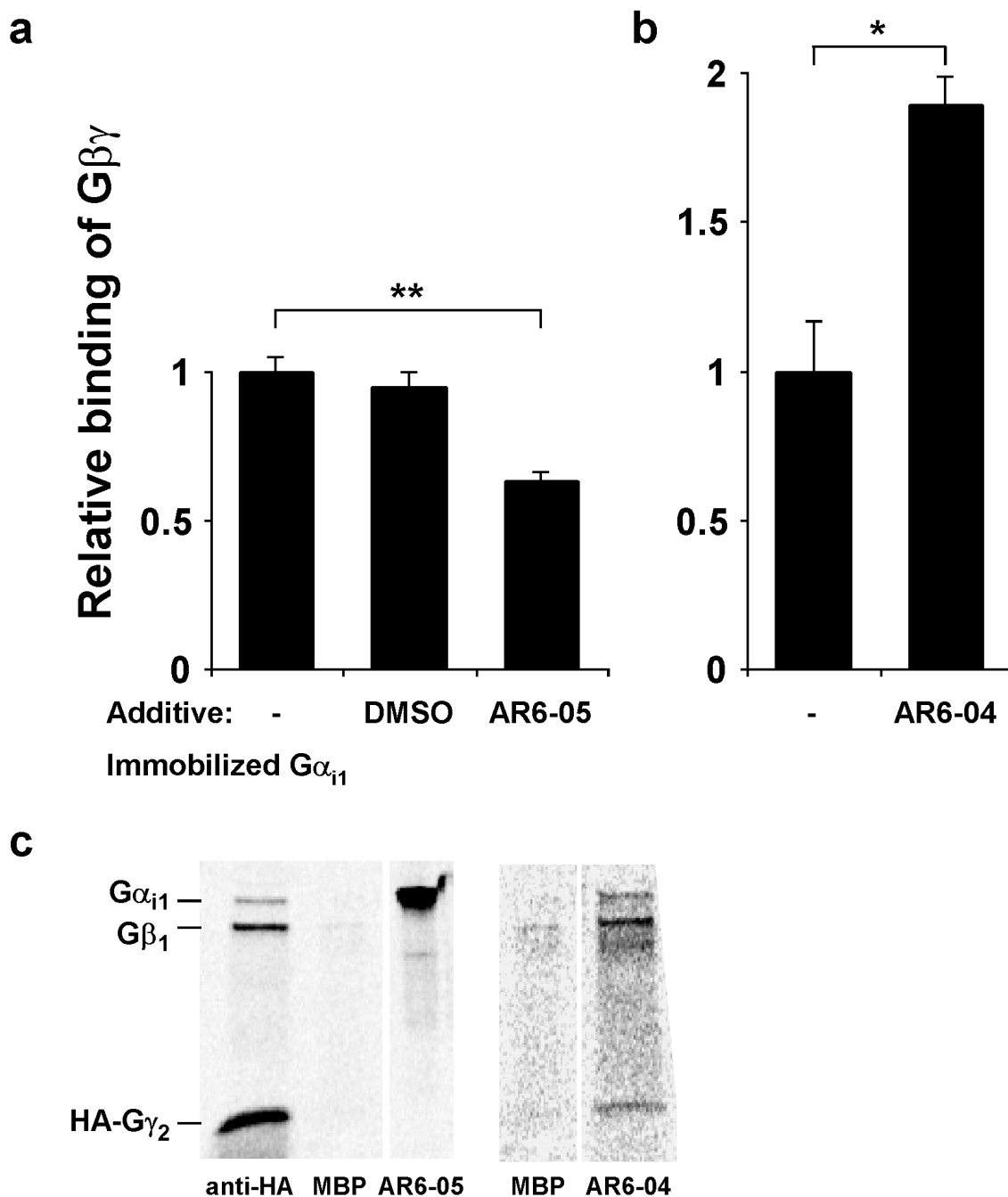


Figure 2. AR6-04 and AR6-05 $G\alpha_{i1}$ -binding peptides differentially affect $G\beta\gamma$ association. **(a)** and **(b)** Binding of ^{35}S -Met-labeled $G\beta_1\gamma_2$ to immobilized $G\alpha_{i1}$ in the presence or absence of AR6-05 (20 μM) or AR6-04 (33 μM). AR6-05 competes with $G\beta\gamma$ for association to $G\alpha_{i1}$ ($n = 4$, $p = 0.0050$) while AR6-04 increases $G\beta\gamma$ binding ($n = 3$, $p = 0.041$). DMSO (~1%, vol/vol) had no effect on $G\beta\gamma$ binding ($n = 3$, $p = 0.50$). **(c)** Binding of ^{35}S -Met-labeled $G\alpha_{i1}\beta_1\gamma_2$ to immobilized peptides. Anti-hemagglutinin (HA) antibody immunoprecipitates the HA-tagged $G\gamma_2$ subunit and confirms the presence of reconstituted heterotrimers. Immobilized maltose-binding protein (MBP) fails to pull down G proteins while binding of $G\alpha_{i1}$ to immobilized AR6-05-MBP completely precludes $G\beta_1\gamma_2$ association. AR6-04-MBP, however, pulls down

the intact heterotrimer. The control MBP lane is shown again at the same contrast as the AR6-04 lane for comparison.

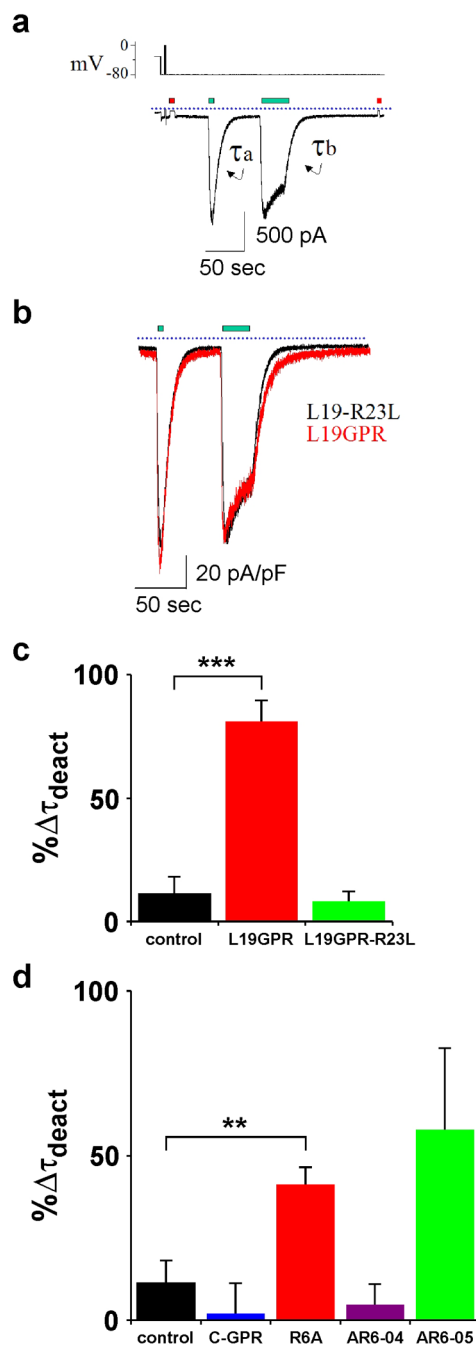


Figure 3. Effect of intracellular application of peptides on GIRK deactivation kinetics. **(a)** HEK293 cells stably expressing GIRK1 and 2 and the dopamine receptor D_{2s} were recorded by whole-cell patch-clamp (see Methods). Zero-K⁺ buffer (red bar) was perfused for 4 sec to determine GIRK basal activity. Application of dopamine for 4 and 30 sec (green bars) activated GIRK currents. Dopamine washout was followed by GIRK channel deactivation. τ_a and τ_b are the GIRK deactivation time constants following the short and long dopamine applications, respectively. The dotted line represents 0 pA. **(b)** Superposition of representative current traces of cells recorded in the presence of 2 μ M of the control peptide L19GPR-R23L (black) or the L19GPR peptide (red). L19GPR-R23L is a negative control peptide which contains a mutation to a

critical Arg residue (26). Current traces were normalized to cell membrane capacitance and current amplitude in Zero-K⁺ buffer was subtracted from current traces in High-K⁺ buffer. **(c)** L19GPR (2 μM) increases τ_b after prolonged dopamine application ($n = 7$, $p = 3.9 \times 10^{-5}$) while the control L19GPR-R23L peptide (2 μM) has no effect ($n = 2$, $p = 0.71$). % $\Delta\tau_{\text{deact}}$ is the percentage change of τ_b from τ_a . **(d)** R6A (100 μM) moderately increases τ_b ($n = 4$, $p = 0.0065$) while AR6-04 (40 μM, $n = 5$, $p = 0.49$) and the control C-GPR peptide (100 μM, $n = 5$, $p = 0.44$) have no effect. AR6-05 (40 μM) appears to increase τ_b ($n = 5$, $p = 0.13$) but there is significantly increased error in the kinetics measurements likely due to the effect that AR6-05 has on basal GIRK activity. In **(c)** and **(d)**, the control contains <0.5% (v/v) DMSO.

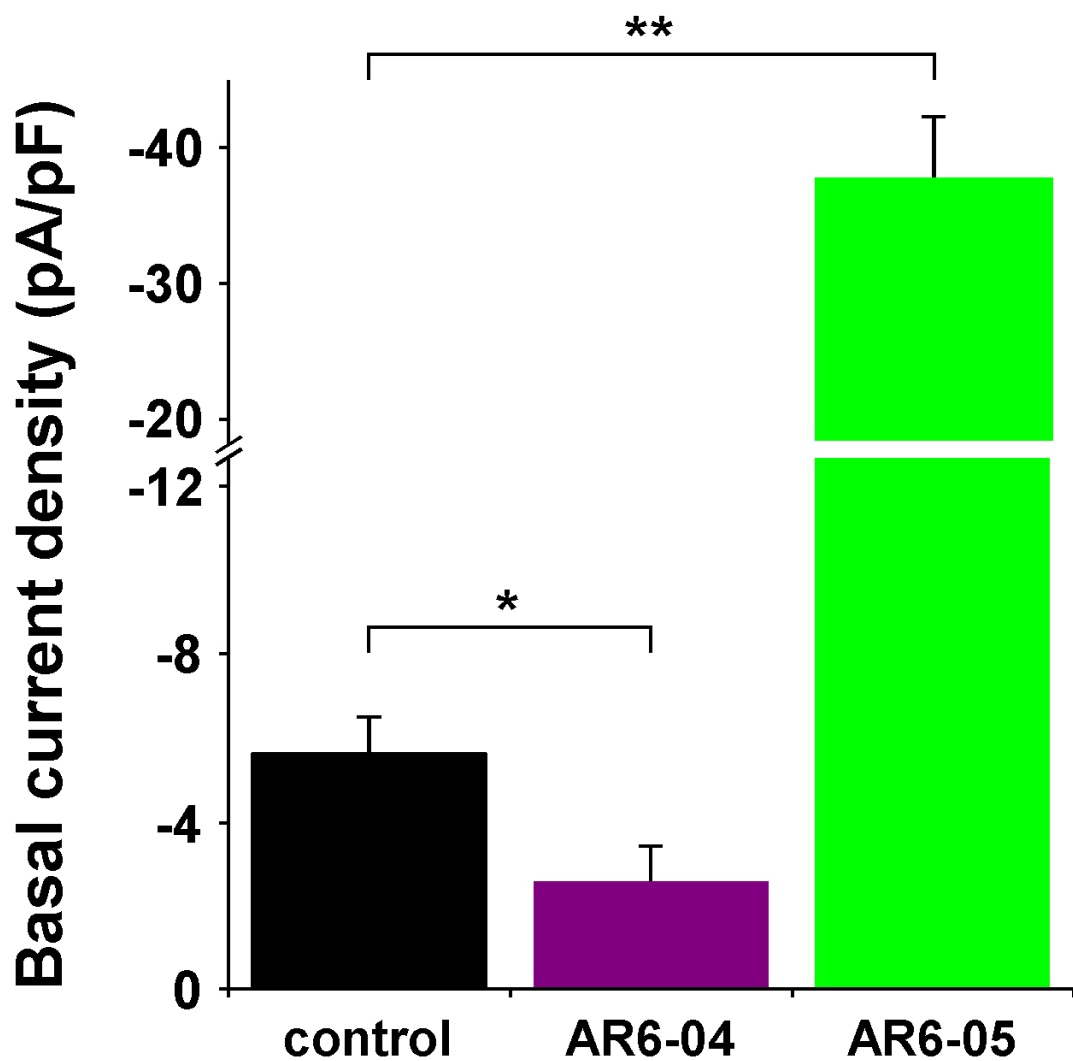


Figure 4. Intracellular application of 40 μ M AR6-05 or AR6-04 increases ($n = 4$, $p = 0.0046$) or decreases ($n = 5$, $p = 0.027$) basal GIRK currents, respectively. Current densities are determined by normalization with the individual cell capacitance. The control contains <0.5% (v/v) DMSO.